

---

# SKIN LESION SEGMENTATION AND CLASSIFICATION USING DEEP LEARNING AND HANDCRAFTED FEATURES

---

A PREPRINT

**Redha Ali**

Department of Electrical and Computer Engineering  
University of Dayton  
300 College Park, Dayton, Ohio 45469  
almahdir1@udayton.edu

**Hussin K. Ragb**

Department of Electrical and Computer Engineering  
Christian Brothers University  
Memphis, Tennessee  
hragb@cbu.edu

December 21, 2021

## ABSTRACT

Accurate diagnostics of a skin lesion is a critical task in classification dermoscopic images. In this research, we form a new type of image features, called hybrid features, which has stronger discrimination ability than single method features. This study involves a new technique where we inject the handcrafted features or feature transfer into the fully connected layer of Convolutional Neural Network (CNN) model during the training process. Based on our literature review until now, no study has examined or investigated the impact on classification performance by injecting the handcrafted features into the CNN model during the training process. In addition, we also investigated the impact of segmentation mask and its effect on the overall classification performance. Our model achieves an 92.3% balanced multiclass accuracy, which is 6.8% better than the typical single method classifier architecture for deep learning.

**Keywords** Medical imaging, deep learning, skin cancer, dermoscopic images, skin cancer classification, network fusion

## 1 Introduction

Skin cancer is a cancer type that has a significant impact on society in the United States and across the world. The American Cancer Society's report in the year 2019 estimated that 96,480 new cases of melanoma are expected (57,220 in male and 39,260 in female), and 7,230 people will die of melanoma (4,740 males and 2,490 female) [1]. Therefore, to decrease the number of deaths, scientists and researchers have made a tremendous effort to reduce the impact of skin cancer. An early stage of melanoma detection increases one's survival rate (99% if diagnosed in Stage I) in the United States. However, when the disease reaches the lymph nodes, the survival rate decreases to 63% and if further decreases to 20% when the disease spreads to distant organs [2, 3].

To aid patients in spotting melanoma, dermatologists recommend the use of the ABCDE rule. The ABCD rule was introduced in [4] in 1985 as the ABCDE rule and then extended to the ABCDE rule in 2004 [5] and involves some key features of melanoma. However, the accuracy of unaided visual inspection is about 60% [6]. The accurate diagnosis of the skin lesion is by taking a biopsy specimen where it enables the pathological analysis to differentiate between different types of the disease. However, this type of analysis is not always possible, and it is both time and labor-intensive [7]. Recently, medical professionals have used dermoscopy, a new imaging technology that helps dermatologists to diagnose skin lesions more accurately than the unaided eye. Dermoscopy is a microscopy-based diagnostic method, and it is a non-invasive Imaging Techniques[8]. Dermoscopy images generate a large amount of detailed images of skin cancer, and magnify the skin and eliminate surface reflection. However, the results of several studies have shown that an expert dermatologist can achieve a diagnostic accuracy between roughly 75% to 84% [6, 9]. The risk of the wrong diagnosis can be increased with the lack of experience; this leads to interest in using artificial intelligence and machine learning to develop a Computer-Aided Diagnosis (CAD) system that provides a second opinion to help the dermatologist.

The architecture of a skin cancer CAD system typically consists of three stages: (i) Lesion Segmentation, (ii) Attribute Detection, (iii) Disease Classification. Our contribution focuses only on the first and third stages. The International Skin Imaging Collaboration (ISIC) is an academic and industry partnership designed to improve melanoma diagnosis, sponsored by the International Society for Digital Imaging of the Skin (ISDIS). The ISIC archive holds the most extensive publicly available dataset of dermoscopy images of skin lesions. The ISIC organization will benefit from the use of state-of-the-art machine learning technology.

Computer vision and machine learning have progressed rapidly and played an important role in the medical field, including medical image segmentation, detection, and classification [10, 11, 12, 13, 14]. Convolutional neural networks (CNN) [15] are a type of widely used deep artificial neural network. CNNs outperform the state-of-the-art in several computer vision applications [16, 17]. CNN have also been presented in the field of medical image analysis [16]. Several automated CAD system papers have been presented in the literature [18, 19, 20, 21, 22, 23, 24, 25]. Moreover, various ensemble systems have proven very practical and versatile in medical image analysis domains and real-world applications [26, 19, 24, 22, 27]. However, there is still an opportunity for further development in the accuracy of its diagnosis.

In this research, we propose an algorithm for skin cancer segmentation and classification at a more treatable stage. Our proposed approach is computationally efficient and combines information from both deep learning and handcrafted features. We develop hybrid features, a new type of image feature, which has a more solid discrimination ability than single method features. This study involves a new technique that will inject the handcrafted features into the fully connected layer of the CNN model during the training process and enhance the segmentation model for better-handcrafted features.

## 2 Materials and Methods

### 2.1 Dataset

The International Skin Imaging Collaboration (ISIC) is an academic and industrial partnership designed to aid in melanoma detection, sponsored by the International Society for Digital Imaging of the Skin (ISDIS) [20]. The ISIC archive owns the most comprehensive publicly available dataset of dermoscopy images of skin lesions [28]. In this study, we used the 2018 challenge dermoscopy databases to train and evaluate our proposed model. The segmentation dataset consists of 2,594 skin lesion images with corresponding ground truth for training. Also, there are around 100 samples for validation and 1,000 samples for testing. However, the ground truth masks for validation and testing images are not provided. The training dataset for the classification task consists of 10015 images. The images are 8-bit RGB dermoscopy images ranging from  $540 \times 722$  to  $4499 \times 6748$  pixels.

### 2.2 Data pre-processing and augmentation

The preprocessing step is performed using color constancy, the Shades of Gray method, introduced by Finlayson [29]. We applied this approach on all images during training and testing as a preprocessing step with norm  $p=6$ . Preprocessing is crucial to normalize images across datasets where acquiring the images uses an unknown light source. Hence, we want to make all images appear identical to colors under canonical light. We used online data augmentations to prevent our model from overfitting and to improve performance and outcomes of our model. Also, data augmentations reduce the effect of the small dataset. We performed data augmentation on all datasets during training and testing. Data augmentation included random crops, random rotation ( $0 - 180^\circ$ ), vertical and horizontal flips, and shear ( $0 - 30^\circ$ ). All augmentation hyperparameters were selected randomly. Figure 1 shows examples of skin lesion images after preprocessing. Finally, Each image is resized to fit the input of ResNet50[30], and DenseNet201 [31] with an image input size of  $224 \times 224$  pixels.

### 2.3 Segmentation Model

We utilizes an ensemble of two new deep learning architectures which introduced in [19], including VGG19-UNet, and DeeplabV3+. The illustration of our ensemble structure for lesion segmentation is shown in Fig. 2. The architecture details of VGG19-UNet and DeeplabV3+ described in [19]. The VGG19-UNet and DeeplabV3+ models were trained using Dice coefficient loss (also known as Srensen-Dice similarity coefficient). The Dice coefficient loss is based on the Srensen-Dice similarity coefficient for measuring overlap between two segmented images. In the ensemble technique, we employed an unweighted average where the probability matrices have been averaged to form the final predicated segmented mask for every dermoscopy image. The ensemble approach is shown in Fig. 2.

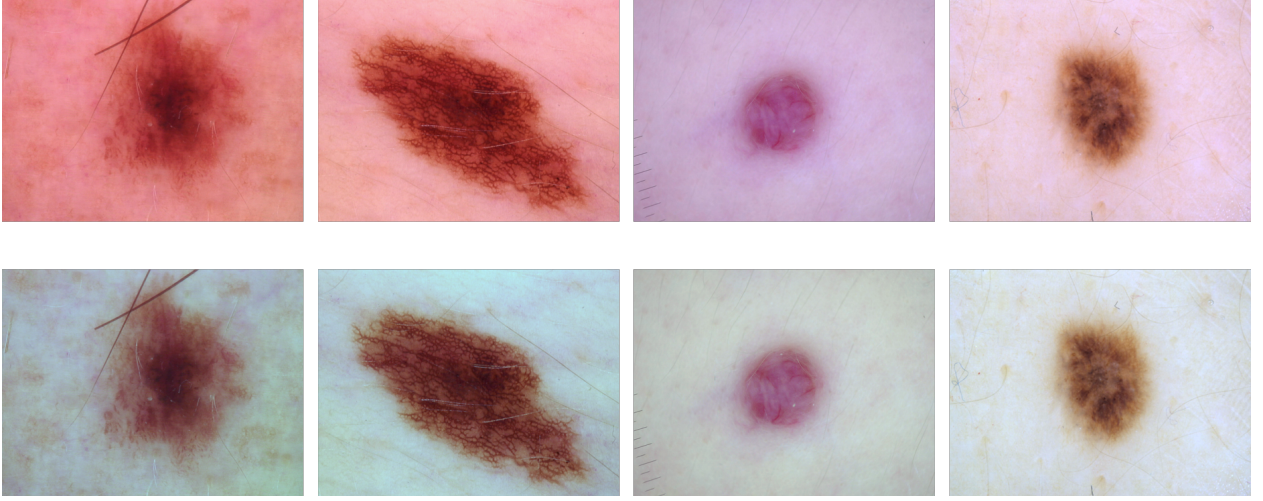


Figure 1: Examples of skin lesion images after preprocessing: (top) raw images, (bottom) image obtained using color constancy.

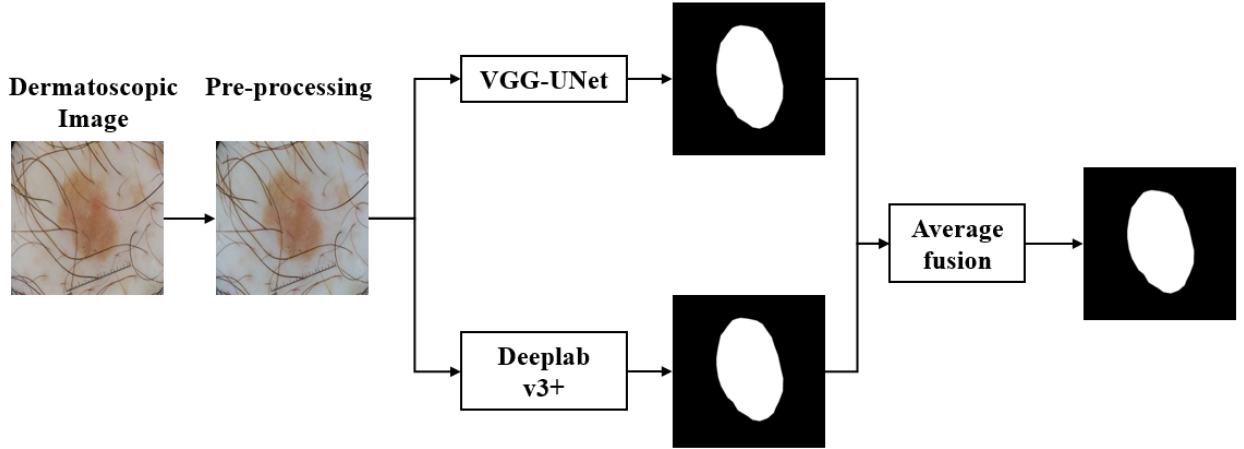


Figure 2: Illustration of our ensemble framework for lesion segmentation.

## 2.4 Handcrafted Features

For each detected and segmented lesion, the handcrafted features listed in [32] are computed. The features are computed from the RGB image along with the lesion segmentation mask obtained using the method in segmentation model 2.3 above. The features employed are similar to those used in [32]. However, here they are computed for each of the three color channels and concatenated. The 200 geometric features are computed based on the shape and position information provided by the final segmentation mask.

## 2.5 Classification Models

In this paper, we developed a novel and efficient deep learning training strategy to train a signal CNN model with both raw image and handcrafted features. The proposed hybrid model is illustrated in Fig. 3. The overall hybrid model consists of two core modules: (i) ensemble segmentation model and 200 handcrafted features. (ii) transfer learning using pre-trained CNN architecture with the minor modification allows the pre-trained CNN to utilize both raw image and handcrafted features. To begin, we first segment all pre-processed dermoscopic images using our ensemble segmentation model to compute the 200 handcrafted features. We then use those computed features to fine-tune the pre-trained models along with the pre-processed dermoscopic images. Our model used two pre-trained models,

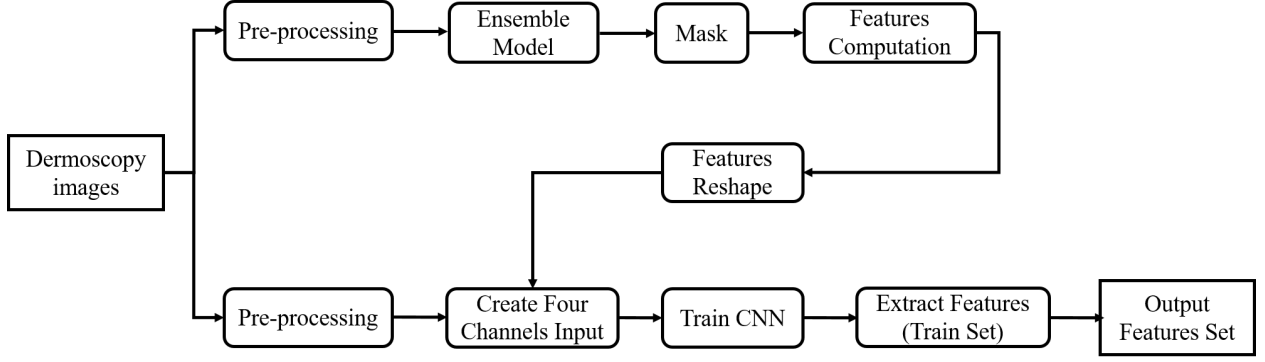


Figure 3: Illustration of our ensemble framework for lesion classification.

Table 1: Network models

Network	Depth	Parameters (Millions)	Image Input Size
ResNet50	50	25.6	224 x 224
DenseNet201	201	20	224 x 224

including ResNet-50 and DenseNet-201. We concatenate the features that the last convolution layer has produced with handcrafted features in channel dimensions. Then, we inject the handcrafted features into the fully connected layers during the training and fine-tune the pre-trained models. Finally, we extracted the features from both models and fed them to SVM for final predictions.

## 2.6 Evaluation Metrics

It is important to assess the efficacy of classification algorithms to aid in method comparisons, method selection, understanding system limitations, and to identify opportunities for future improvement. The metrics we use as performance and efficiency metrics is balanced accuracy (**BACC**) specificity (**SPEC**), sensitivity (**SENS**), **Accuracy**, and the area under the curve (AUC) for the receiver operating characteristic (ROC) curve. These metrics provide an objective quantitative picture of the efficacy of the systems tested.

The classification problem studied in this paper is multi-class classification. Thus, each exemplar fits into one of four subsets:

1. True positive (TP): Interpreted as the classifier correctly predicts the positive sample.
2. True negative (TN): Interpreted as the classifier correctly predicts the negative sample.
3. False positive (FP): Interpreted as the classifier incorrectly predicts the positive sample.
4. False negative (FN): Interpreted as the classifier incorrectly predicts the negative sample.

Based on the cardinality of these subsets, we can calculate the statistical quantities for each metric as follows:

$$\text{BACC} = \frac{(TN/(TN + FP)) + (TP/(TP + FN))}{2}, \quad (1)$$

$$\text{SPEC} = \frac{TN}{(TN + FP)}, \quad (2)$$

$$\text{SENS} = \frac{TP}{(TP + FN)}. \quad (3)$$

and

$$\text{Accuracy} = \frac{TP + TN}{(TP + TN + FP + FN)}. \quad (4)$$

On the other hand, the AUC metric[33] is the area under the ROC curve and it captures the degree of separability between classes. The higher AUC score represents a better model efficiency and vice versa.

Table 2: Shows the hold-out validation distribution of the dataset and the number of training, validation, and testing examples

Disease Categories	Image Input Size	No. of training set	No. of testing set
Actinic keratosis	224 x 224	229	98
Basal cell carcinoma	224 x 224	360	154
Benign keratosis	224 x 224	769	330
Dermatofibroma	224 x 224	81	34
Melanocytic nevus	224 x 224	4694	2011
Melanoma	224 x 224	779	334
Vascular lesion	224 x 224	99	43
Total	-	7011	3004

### 3 Results and Discussion

As mentioned, the reported results are based on the 3004 test images of the ISIC 2018 skin lesion classification challenge. Since the ground truth of the testing dataset was not provided by the challenge organizers, We randomly split the dataset into 70% for training and 30% for testing examples for each class. Then, we divided the training dataset into 90% and 10% for training and validation sets. Table 2 shows the hold-out validation distribution of the ISIC 2018 skin lesion dataset and the number of training and testing samples.

Table 3 shows the performance metrics for our approaches, including the proposed hybrid model and the ensemble of the hybrid models, with two baseline models for skin lesion classification using dermoscopic images. Note that the ensemble of the hybrid models obtained the highest BACC (92.3%), outperforming the hybrid model and baseline models in this experiment. Furthermore, note that the hybrid model trained with handcrafted features outperforms the baseline models. Note that indicates the proposed hybrid training strategy is very effective and improved the balanced accuracy of ResNet-50 and DenseNet-201 by 3% and 3.9%, respectively.

Table 3: Comparison of the proposed model with the baseline models ResNet-50 and DenseNet-201

Models	BACC	SPEC	SENS	Accuracy	AUC
ResNet-50	85.2%	96.1%	74.3%	96.3%	0.974
DenseNet-201	85.5%	95.7%	75.2%	95.8%	0.968
Hybrid ResNet-50	88.2%	96.5%	79.9%	96.0%	0.974
Hybrid DenseNet-201	89.4%	96.8%	82.0%	96.5%	0.976
Ensemble	92.3%	97.1%	87.5%	95.4%	0.977

In deep learning, the technique of combining multiple CNNs to form an ensemble is commonly used to improve performance. However, the main contribution of this paper is to investigate the effect of injecting the handcrafted features to the pre-trained CNN during the training that achieves outstanding classification performance on the ISIC 2018 challenge dataset. Moreover, our proposed ensemble hybrid training strategy showed that fusing two networks remarkably improves classification performance.

### 4 Conclusion

Early, affordable, and rapid detection of skin cancer is essential at the early stages to increase one’s survival rate. We successfully proposed an effective classifier for a dermoscopic image as a first-line triage tool to aid patients in spotting melanoma at early stages by training deep transfer learning models using our hybrid training method and combining their outputs into the ensemble. We show that our proposed method exceeds the baseline networks where transfer learning is used. Further research can be conducted by testing new convolutional neural network architectures or with different ensemble techniques.

### References

- [1] American Cancer Society. Cancer facts & figures 2019, vol. 2019. *American Cancer Society Atlanta, GA*, 2019.
- [2] A Staff. Cancer facts & figures 2018. *Atlanta: American Cancer Society, Cancer*, pages 19–20, 2018.
- [3] Andre Esteva, Brett Kuprel, Roberto A Novoa, Justin Ko, Susan M Swetter, Helen M Blau, and Sebastian Thrun. Dermatologist-level classification of skin cancer with deep neural networks. *Nature*, 542(7639):115–118, 2017.

- [4] Robert J Friedman, Darrell S Rigel, and Alfred W Kopf. Early detection of malignant melanoma: the role of physician examination and self-examination of the skin. *CA: a cancer journal for clinicians*, 35(3):130–151, 1985.
- [5] Naheed R Abbasi, Helen M Shaw, Darrell S Rigel, Robert J Friedman, William H McCarthy, Iman Osman, Alfred W Kopf, and David Polsky. Early diagnosis of cutaneous melanoma: revisiting the abcd criteria. *Jama*, 292(22):2771–2776, 2004.
- [6] Harold Kittler, H Pehamberger, K Wolff, and MJTIO Binder. Diagnostic accuracy of dermoscopy. *The lancet oncology*, 3(3):159–165, 2002.
- [7] Amirreza Mahbod, Gerald Schaefer, Isabella Ellinger, Rupert Ecker, Alain Pitiot, and Chunliang Wang. Fusing fine-tuned deep features for skin lesion classification. *Computerized Medical Imaging and Graphics*, 71:19–29, 2019.
- [8] G Argenziano, HP Soyer, V De Giorgi, D Piccolo, P Carli, M Delfino, et al. Dermoscopy: a tutorial. *EDRA, Medical Publishing & New Media*, 16, 2002.
- [9] ME Vestergaard, PHPM Macaskill, PE Holt, and SW Menzies. Dermoscopy compared with naked eye examination for the diagnosis of primary melanoma: a meta-analysis of studies performed in a clinical setting. *British Journal of Dermatology*, 159(3):669–676, 2008.
- [10] Muhammad Imran Razzak, Saeeda Naz, and Ahmad Zaib. Deep learning for medical image processing: Overview, challenges and the future. In *Classification in BioApps*, pages 323–350. Springer, 2018.
- [11] Redha Ali, Russell Hardie, and Almabrok Essa. A leaf recognition approach to plant classification using machine learning. In *NAECON 2018-IEEE National Aerospace and Electronics Conference*, pages 431–434. IEEE, 2018.
- [12] Hussin K Ragb and Vijayan K Asari. Histogram of oriented phase (hop): a new descriptor based on phase congruency. In *Mobile Multimedia/Image Processing, Security, and Applications 2016*, volume 9869, page 98690V. International Society for Optics and Photonics, 2016.
- [13] Hussin K Ragb and Vijayan K Asari. Histogram of oriented phase and gradient (hopg) descriptor for improved pedestrian detection. *Electronic Imaging*, 2016(3):1–6, 2016.
- [14] Hussin K Ragb and Vijayan K Asari. Multi-feature fusion and pca based approach for efficient human detection. In *2016 IEEE Applied Imagery Pattern Recognition Workshop (AIPR)*, pages 1–6. IEEE, 2016.
- [15] Yann LeCun, Léon Bottou, Yoshua Bengio, and Patrick Haffner. Gradient-based learning applied to document recognition. *Proceedings of the IEEE*, 86(11):2278–2324, 1998.
- [16] Karen Simonyan and Andrew Zisserman. Very deep convolutional networks for large-scale image recognition. *arXiv preprint arXiv:1409.1556*, 2014.
- [17] Tom Brosch, Youngjin Yoo, David KB Li, Anthony Traboulsee, and Roger Tam. Modeling the variability in brain morphology and lesion distribution in multiple sclerosis by deep learning. In *International Conference on Medical Image Computing and Computer-Assisted Intervention*, pages 462–469. Springer, 2014.
- [18] Song-Toan Tran, Ching-Hwa Cheng, Thanh-Tuan Nguyen, Minh-Hai Le, and Don-Gey Liu. Tmd-unet: Triple-unet with multi-scale input features and dense skip connection for medical image segmentation. In *Healthcare*, volume 9, page 54. Multidisciplinary Digital Publishing Institute, 2021.
- [19] Redha Ali, Russell C Hardie, Barath Narayanan Narayanan, and Supun De Silva. Deep learning ensemble methods for skin lesion analysis towards melanoma detection. In *2019 IEEE National Aerospace and Electronics Conference (NAECON)*, pages 311–316. IEEE, 2019.
- [20] Yuexiang Li and Linlin Shen. Skin lesion analysis towards melanoma detection using deep learning network. *Sensors*, 18(2):556, 2018.
- [21] Redha Ali, Russell C Hardie, Manawaduge Supun De Silva, and Temesguen Messay Kebede. Skin lesion segmentation and classification for isic 2018 by combining deep cnn and handcrafted features. *arXiv preprint arXiv:1908.05730*, 2019.
- [22] Hussin K Ragb, Ian T Dover, and Redha Ali. Deep convolutional neural network ensemble for improved malaria parasite detection. In *2020 IEEE Applied Imagery Pattern Recognition Workshop (AIPR)*, pages 1–10. IEEE, 2020.
- [23] Nguyen Hong Quang et al. Automatic skin lesion analysis towards melanoma detection. In *2017 21st Asia Pacific symposium on intelligent and evolutionary systems (IES)*, pages 106–111. IEEE, 2017.
- [24] Redha Ali, Russell C Hardie, and Hussin K Ragb. Ensemble lung segmentation system using deep neural networks. In *2020 IEEE Applied Imagery Pattern Recognition Workshop (AIPR)*, pages 1–5. IEEE, 2020.

- [25] Russell C Hardie, Redha Ali, Manawaduge Supun De Silva, and Temesguen Messay Kebede. Skin lesion segmentation and classification for isic 2018 using traditional classifiers with hand-crafted features. *arXiv preprint arXiv:1807.07001*, 2018.
- [26] Redha Ali and Hussin K Ragb. Fused deep convolutional neural networks based on voting approach for efficient object classification. In *2019 IEEE National Aerospace and Electronics Conference (NAECON)*, pages 335–339. IEEE, 2019.
- [27] Barath Narayanan Narayanan, Vignesh Krishnaraja, and Redha Ali. Convolutional neural network for classification of histopathology images for breast cancer detection. In *2019 IEEE National Aerospace and Electronics Conference (NAECON)*, pages 291–295. IEEE, 2019.
- [28] P Tschandl, C Rosendahl, and H Kittler. The ham10000 dataset, a large collection of multi-source dermatoscopic images of common pigmented skin lesions. 2018; sci data (5): 180161, 2018.
- [29] Graham D Finlayson and Elisabetta Trezzi. Shades of gray and colour constancy. In *Color and Imaging Conference*, volume 2004, pages 37–41. Society for Imaging Science and Technology, 2004.
- [30] Sergey Zagoruyko and Nikos Komodakis. Wide residual networks. *arXiv preprint arXiv:1605.07146*, 2016.
- [31] Gao Huang, Zhuang Liu, Laurens Van Der Maaten, and Kilian Q Weinberger. Densely connected convolutional networks. In *Proceedings of the IEEE conference on computer vision and pattern recognition*, pages 4700–4708, 2017.
- [32] Temesguen Messay, Russell C Hardie, and Steven K Rogers. A new computationally efficient cad system for pulmonary nodule detection in ct imagery. *Medical image analysis*, 14(3):390–406, 2010.
- [33] Andrew P Bradley. The use of the area under the roc curve in the evaluation of machine learning algorithms. *Pattern recognition*, 30(7):1145–1159, 1997.